JOURNAL OF APPLIED ELECTROCHEMISTRY 23 (1993) 1207–1213

Kinetics of the electroreduction of anodically formed cadmium oxide layers in alkaline solutions

J.I. DE URRAZA, C.A. GERVASI*, S.B. SAIDMAN‡, J.R. VILCHE

Instituto de Investigaciones Fisicoquímicas Teóricas y Aplicadas (INIFTA), Facultad de Ciencias Exactas, Universidad Nacional de La Plata, Sucursal 4, Casilla de Correo 16, (1900) La Plata, Argentina

Received 18 January 1993; revised 20 April 1993

The kinetics of the potentiostatic electroreduction of cadmium oxide layers on polycrystalline cadmium electrodes have been investigated in 0.01–1.0 M NaOH solutions. The study was undertaken to determine the influence of passive film formation conditions on the electroreduction process of the anodically produced hydrous cadmium hydroxide-oxide layers. By properly adjusting the electroreduction conditions the cathodic potentiostatic current transients can be satisfactorily described by a nucleation and growth mechanism involving the participation of soluble Cd(II) and passivating anodic species. Experimental data were analysed by the application of non linear least squares fit routines. From the parametric identification procedure coherent potential dependencies of the corresponding fitting parameters as well as reasonable values of the physicochemical constants included in the reaction model, have been obtained. In this way it is possible to correlate kinetic data of the electroreduction process of the anodic oxide layers to make a discrimination between the different mechanistic contributions to this complex reaction involving several steps.

1. Introduction

The study of the electroformation and electroreduction of porous hydrous oxide films on cadmium electrodes in alkaline media has been carried out mainly in relation to the electrochemical behaviour of rechargeable active materials in Ni–Cd battery cells [1–7]. For both electrodes the kinetics of the charge/discharge processes are influenced by both short time and large time range ageing effects. Cadmium anodization in alkaline aqueous solutions comprises the formation of a passivating layer consisting of $Cd(OH)_2$ and CdO and the simultaneous generation of soluble Cd(II) species going into solution [6, 8, 9]. The electroreduction of these surface layers furnishes a reduced cadmium overlayer whose properties clearly depend on the applied potential routine during the previous anodic bias. The kinetics of the voltammetric electroreduction process have been tentatively explained through a nucleation and growth mechanism, although additional experimental information was required for deriving a more sound conclusion [6]. This opens the possibility of investigating further the electroreduction of anodically formed passive layers on cadmium electrodes in alkaline media.

The aim of the present paper is to provide a new insight into the probable reaction mechanism using appropriate perturbing potential programs to generate the passivating cadmium oxide layer and following the kinetics of the electroreduction reaction under preset constant applied potentials.

2. Experimental details

The experimental setup was described in previous publications [6, 10, 11]. 'Specpure' cadium (Johnson Matthey Chemicals Ltd) in the form of rotating discs (0.20 cm^2 apparent area) axially mounted in PTFE holders were used as working electrodes in x M NaOH, $0.1 \leqslant x \leqslant 1.0$, at 25°C, under purified nitrogen gas saturation. Potentials were measured against a SCE properly shielded, but in the text they are referred to the NHE scale. Cadmium electrodes were mechanically polished with 400 and 600 grade emery papers and 1.0 and 0.3 μm grit alumina-acetone suspensions, and afterwards thoroughly rinsed in triply-distilled water. Finally, cadmium electrodes were cathodically polarized for 5 min at potentials in the net HER range to achieve a reproducible electroreduced Cd surface. Subsequently, the electrodes were subjected to linear potential scans between cathodic ($E_{s,c}$) and anodic ($E_{s,a}$) switching potentials suitable to produce a net anodic layer on the electrode surface, combined with potential steps, usually two potential steps, covering different preset potential regions. The first potential step (E_i) was applied for a set time (τ), to modify the anodic layer in a preestablished way, i.e. to change the total amount of anodic product and to produce ageing effects in order to

* Permanent address: Centro de Investigación y Desarrollo en Tecnología de Pinturas (CIDEPINT), calle 52 e/121 y 122, (1900) La Plata, Argentina. CIC Researcher.
‡ Permanent address: Instituto de Ingeniería Electroquímica y Corrosión, Universidad Nacional del Sur, (8000) Bahía Blanca, Argentina.

0021-891X

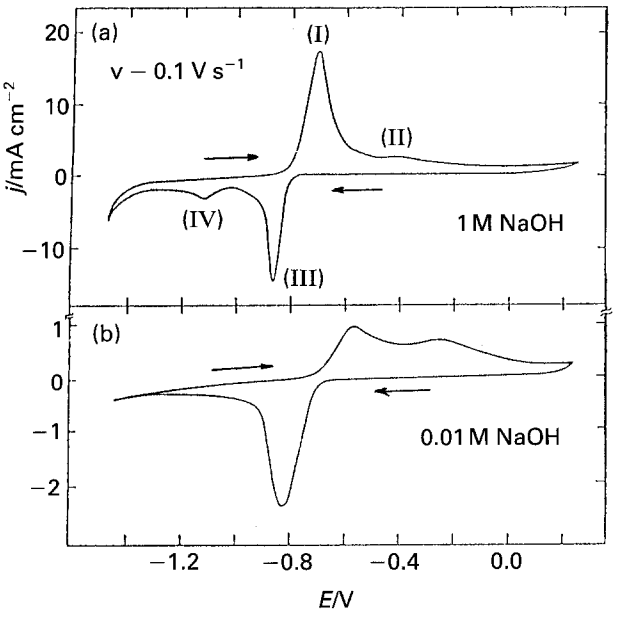

Fig. 1. Influence of the concentration of NaOH solution on the stabilized voltammograms, $v = 0.1\,V\,s^{-1}$; $E_{s,c} = -1.46\,V$. $E_{s,a} = 0.24\,V$. (a) 1.0 M NaOH; (b) 0.01 M NaOH.

vary the ratio of the anodic layer constituents. The second potential step (E_f) was set sufficiently negative to electroreduce the anodic layers, the corresponding transients being systematically recorded. The experiments were made with the electrode kept either still or under rotation and potential routines are displayed as insets in the corresponding figures.

3. Results and discussion

The voltammograms of cadmium in 0.01 M and 1 M NaOH at $v = 0.1\,V\,s^{-1}$ run between $E_{s,c} = -1.46\,V$ and $E_{s,a} = 0.24\,V$ are shown in Fig. 1. In the positive going potential scan the anodic current initiates at a potential close to the $Cd/Cd(OH)_2$ reversible electrode potential and at least two anodic current peaks (I and II) are recorded at more positive potentials. The reverse scan exhibits two cathodic current peaks (III and IV) and a net cathodic current contribution at potentials more negative than −1.1 V. These voltammograms are presented with the purpose of describing the potential ranges of the different electrode

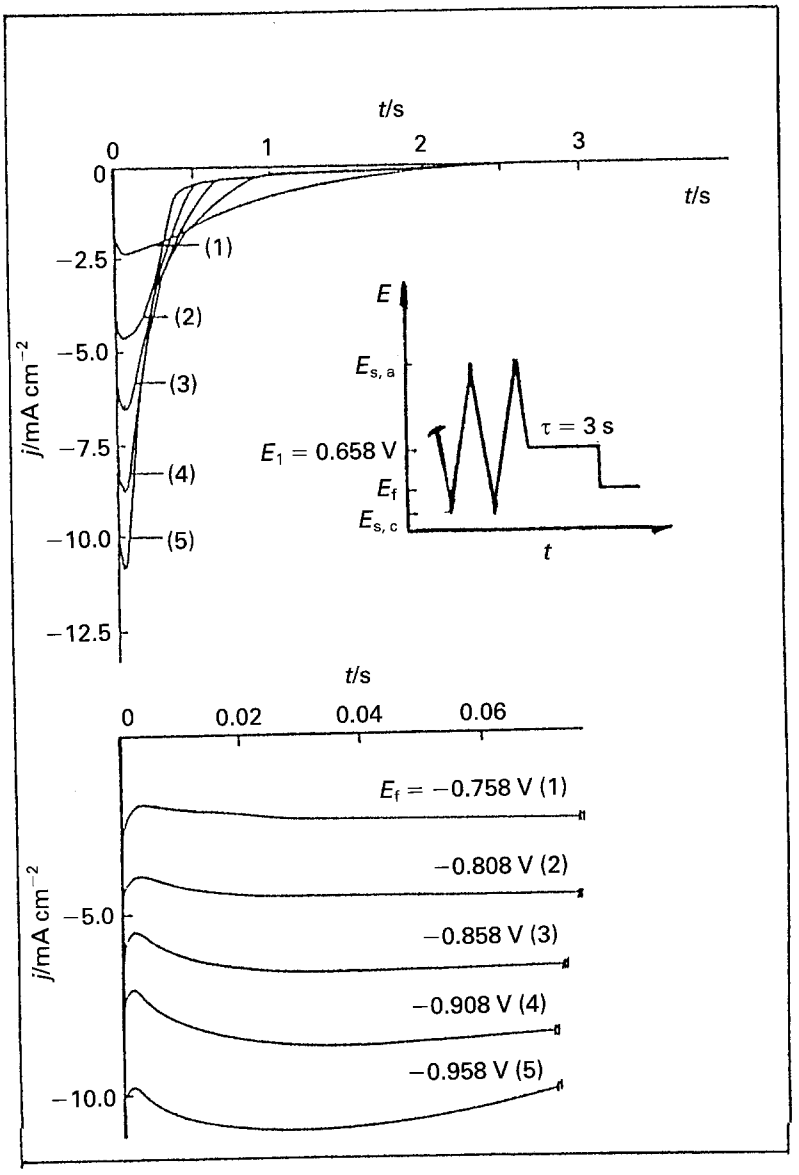

Fig. 2. Cathodic current transients for $E_i = -0.66\,V$ up to different E_f values recorded after attaining the stabilized voltammogram under the following conditions: $v = 0.01\,V\,s^{-1}$, $E_{s,c} = -1.36\,V$, $E_{s,a} = 0.24\,V$.0.1M NaOH.

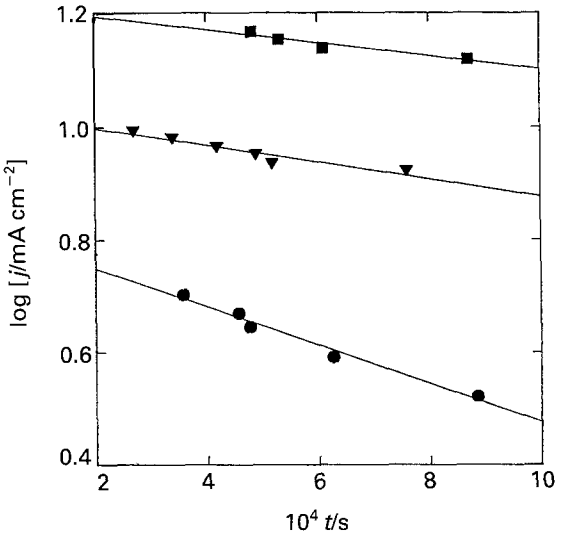

Fig. 3. Plot of $\log j$ against t for the initial falling part of the electroreduction current transients run for $E_i = -0.66$ V up to different E_f: (■) −0.86, (▼) −0.81 and (●) −0.76 V. Points are taken from current transients run as indicated in Fig. 2.

reactions. The nomenclature and the assignments of the current contributions follow that indicated in previous publications referred to cadmium voltammetry in strongly alkaline solutions [6, 8, 12].

The potentiostatic current transients related to the electroreduction of the anodic layer previously formed at preset $E_{s,a}$ values, were analysed by setting E_f in the potential range of peak III (Fig. 2). The j–t curves consist of an initial spike which includes the double layer charging followed by a continuous current decay observable over the first 5 ms to attain a minimum current density. The current transient thereafter rises to display a typical peak j_M at the time t_M whose value is in the order of 100 ms and then decays. The Helmholtz layer capacitance, C_H, was determined from the high frequency impedance data at $E = -0.9$ V and yielded a value of about 35 μF cm^{-2}.

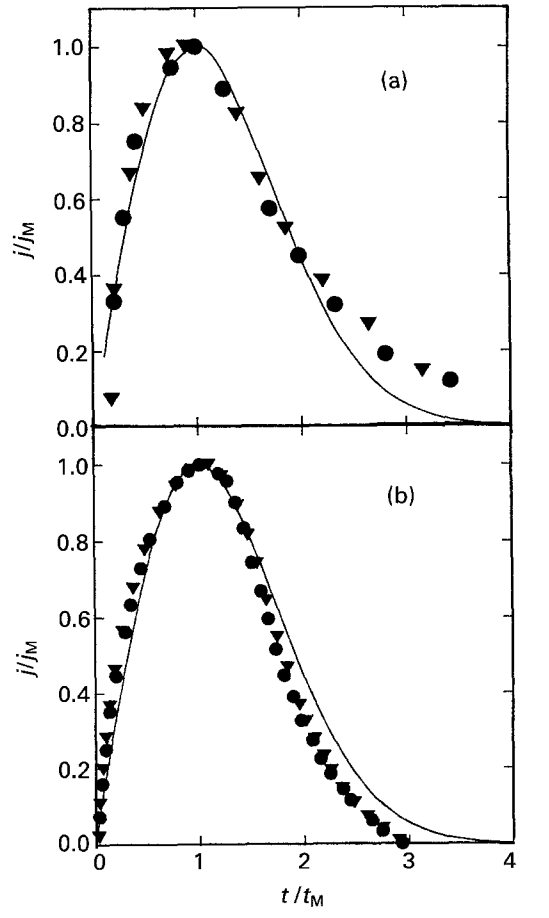

Fig. 4. Reduced variable test plots. Instantaneous nucleation and 2D growth equation (full lines). Points are taken from current transients run at different E_f after correction for the contribution indicated in Fig. 3. (a) 0.01 M NaOH, $E_i = -0.61$ V, $E_f = -0.81$ (●) and −0.86 V (▼); (b) 1 M NaOH, $E_i = -0.76$ V, $E_f = -1.02$ (●) and −1.04 V (▼).

An examination of the initial falling part of the electroreduction current transient, properly corrected for the double layer charging contribution, reveals that the j–t curves in this short time range obey a linear $\log j$ against t relationship (Fig. 3). On the other hand, the rising part of the current transients exhibits a linear j against t relationship when the residual currents from the first current decay process are subtracted. Furthermore, it is interesting to note that such phenomenological behaviour is indeed predicted by the instantaneous nucleation and two-dimensional (2D) growth model, under charge transfer control [13]. A satisfactory indication of the agreement between experimental data and the formalism of the preceding nucleation and growth model is found through the reduced-variable test plot, i.e. j/j_M against t/t_M (Fig. 4(a) and (b)) by taking also into account the residual-current correction. Otherwise, it is worth noting that independently of the selected E_f a nearly constant value of $Q_M/j_M t_M = 0.65 \pm 0.05$ can be calculated in full agreement with the theoretical value already derived from the proposed model which gives 0.648 [14]. Accordingly, the cathodic current transients $j(t)$, can be described by an expression given as the sum of two processes, whose corresponding current contributions are hereby denoted as $j_1(t)$ and $j_2(t)$:

$$j(t) = j_1(t) + j_2(t) \tag{1}$$

where

$$j_1(t) = P_1 t \exp(-P_2 t^2) \tag{2}$$

and

$$j_2(t) = P_3 \exp(-P_4 t) \tag{3}$$

Equation 2 corresponds to the current decay of an instantaneous nucleation and 2D growth process under charge transfer control. In this case, the parameters P_1 and P_2 are given by

$$P_1 = 2zF\pi hMk^2 N_0/\rho \tag{4}$$

and

$$P_2 = \pi M^2 k^2 N_0/\rho \tag{5}$$

where M is the molecular weight of the new phase, k the rate constant for crystal growth parallel to the surface, ρ the density of the surface layer, and h the height

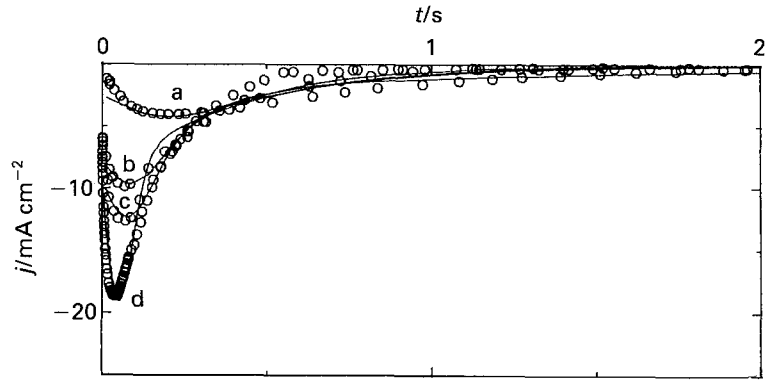

Fig. 5. Experimental current transients (○ symbols) and fitting of these data according to Equation 1 (full traces), 0.01 M NaOH, $E_i = -0.61$ V, at different E_f values. E_f: (a) −0.760, (b) −0.810, (c) −0.860 and (d) −0.910 V.

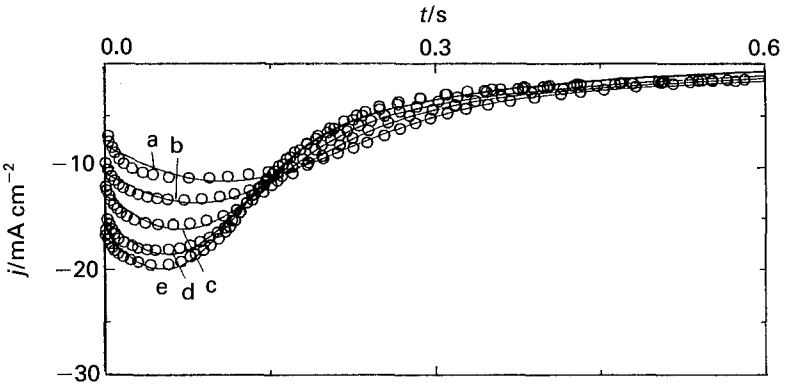

Fig. 6. Experimental current transients (○ symbols) and fitting of these data according to Equation 1 (full traces), 1 M NaOH, $E_i = -0.76$ V, at different E_f values. E_f: (a) −0.980, (b) −1.000, (c) −1.020, (d) −1.040 and (e) −1.060 V.

of the growing layer when N_0 nuclei are instantaneously formed. On the other hand, Equation 3 which describes the initial falling current transient corrected for the double layer charging contribution, can be related, in principle, to an instantaneous nucleation and 2D growth under diffusion control [15]. In this case P_3 and P_4 are explicitly given by the following relationships:

$$P_3 = q_{mon}\pi K_j D_j N_0 \tag{6}$$

$$P_4 = \pi K_j D_j N_0 = P_3/q_{mon} \tag{7}$$

where q_{mon} is the monolayer charge density, D_j the diffusion coefficient, and $K_j = (8\pi c_j M\rho^{-1})^{1/2}$.

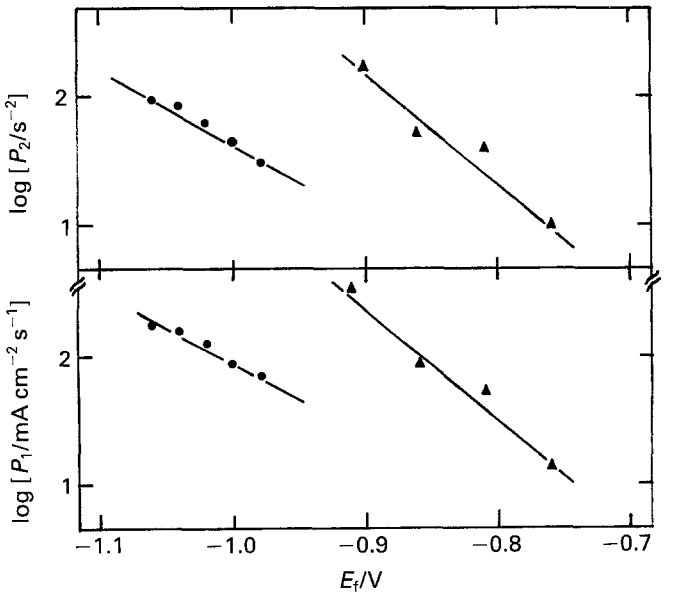

Fig. 7. Dependences of P_1 and P_2 on E_f. Values of P_1 and P_2 derived from the fitting procedure by using Equation 1; (▲) 0.01 M NaOH, $E_i = -0.61$ V; (●) 1 M NaOH, $E_i = -0.76$ V.

Table 1. Parameters used for current transient fitting according to Equation 1 as shown in Figs 5 and 6 (full traces)

E_f /V	P_1 /mA cm^{-2} s^{-1}	P_2 /s^{-2}	P_3 /mA/cm^{-2}	P_4 /s^{-1}
$E_i = -0.61$ V, $\tau = 3$ s, 0.01 M NaOH				
−0.91	326.96	163.7	9.39	2.55
−0.86	85.02	51.5	9.53	2.87
−0.81	51.45	39.5	7.82	2.27
−0.76	14.0	10.0	2.50	0.80
$E_i = -0.76$ V, $\tau = 3$ s, 1 M NaOH				
−1.06	177.8	92.5	16.89	5.37
−1.04	162.3	83.4	15.34	5.04
−1.02	126.2	62.8	12.78	4.07
−1.00	89.3	43.2	10.65	3.42
−0.98	71.3	30.1	7.95	2.63

Figures 5 and 6 show the good agreement between experimental and calculated data, the latter evaluated from Equation 1 with the set of parameters assembled in Table 1. The potential dependencies of P_1 and P_2 are shown in Fig. 7. Irrespective of the E_i value in the range −1.0 to −0.75 V, the slope of log P_i (i = 1, 2) against E_f plots, approaches a common value of 0.12 V dec^{-1} for those transients recorded in NaOH 0.01 M, whereas in 1 M NaOH the slope is about 0.18 V dec^{-1}. The q_{mon} values resulting from the fitting procedure are 2.26 ± 0.15 mC cm^{-2} (0.01 M NaOH) and 2.51 ± 0.15 mC cm^{-2} (1.0 M NaOH). Taking into account an atomic radius of 0.154 nm, the electric charge density corresponding to the reduction of Cd^{2+} to form a monolayer of metal on the (0 0 1) plane is close to 0.4 mC cm^{-2}. The difference between the experimental and the theoretical values of q_{mon}, can be associated with an increase of the effective area due to the surface roughness which implies a roughness factor of about 5. Indeed, the ellipsometric parameters of the electroreduced Cd overlayer are different from those of the initial surface. This fact, which can be correlated to the enhancement of the HER current on this surface, was recently attributed to the development of some microporosity at the cadmium overlayer [8, 12]. The estimation of D_j from equation 7, assuming $N_0 = 10^{-9}$ nuclei cm^{-2}, yields a value in the order of 10^{-6} cm^2 s^{-1} for the measurements performed in the pH range considered in this work.

By using for the Cd^0 overlayer the corresponding M = 112.41 g mol^{-1} and $\rho = 8.65$ g cm^{-3} values, from Equations 4 and 5 it is possible to calculate then the height of the growing layer, $h \simeq 1$ nm. It should be noted that this value is close to the thickness δ of the passivating films formed in the potential range of peak I according to previous *in situ* ellipsometric measurements [8].

Nevertheless it is possible to consider a slight modification of the theoretical model above presented in order to account for the edge profile of the expanding centres which will not be perfect cylinders but will be likely to have bevelled edges [16] (Fig. 8). Thus, the kinetics formalism for a 2D nucleation and growth process under charge transfer control could be better written as follows.

$$j_1^*(t) = P_1^*(t + P_5)\exp[-P_2^*(t + P_5)^2] \quad (8)$$

where

$$P_1^* = P_1\left(\frac{h^2 + \Delta r^2}{h}\right) \quad (9)$$

$$P_2^* = P_2\left(\frac{h^2 + \Delta r^2}{h^2}\right) \quad (10)$$

and

$$P_5 = (\rho/kM)\left(\frac{h\Delta r}{(h^2 + \Delta r^2)^{1/2}}\right) \quad (11)$$

and Δr is the increment in radius compared to the cylindrical geometry as shown in Fig. 8.

Data obtained for current transients in 1 M NaOH correlate satisfactorily (Fig. 9) with the following $j^*(t)$ expression,

$$j^*(t) = j_1^*(t) + j_2(t) \quad (12)$$

and the corresponding adjusting parameters used in Equation 12 are given in Table 2. The calculated layer thickness derived from $h = P_1^*/P_2^*$ using the modified model is $h = 1.64 \pm 0.2$ nm.

It is interesting to note that, alternatively, a relationship such as that presented in Equation 2 could also be assigned to a progressive nucleation and growth of two-dimensional layers controlled by diffusion [15]. Accordingly, $P_1' = q'_{mol}\pi A K_k D_k$ and $P_2' = P_1'/q'_{mon}$, where A denotes the nucleation rate constant (s^{-1} cm^{-2}). By using the values of M and ρ for the Cd^0 layer and assuming a conservative value of $A = 10^6$ s^{-1}, and $c_k = 5 \times 10^{-11}$ mol cm^{-3} and 5×10^{-9} mol cm^{-3} for 0.01 and 1 M NaOH, respectively, it is possible from the above given expression for P_2', to estimate D_k which results about 1.5×10^{-1} cm^2 s^{-1} and 1.5×10^{-2} cm^2 s^{-1}. The assumed values of c_k correspond to the solubilities of $Cd(OH)_2$ through $Cd(OH)_3^-$, which is the most abundant soluble Cd species in the studied pH range and has previously been detected by rrde measurements [17]. Hence, even when the two models are experimentally indistinguishable it seems that the definitions of P_1 and P_2 according to Equations 4 and 5, or its corrected values defined in Equations 9 and 10, are more appropriate to describe the kinetics of the system under consideration.

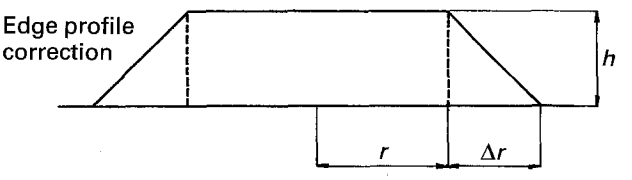

Fig. 8. A schematic representation of the expanding centre and the resulting geometrical quantities after edge profile correction, as proposed in [16].

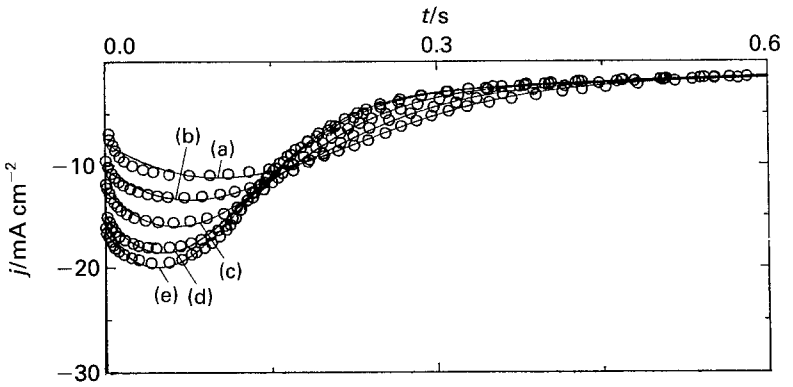

Fig. 9. Fitting of current transients data according to Equation 12 (full traces); 1 M NaOH, $E_i = -0.76$ V at different E_f values. E_f: (a) −0.980, (b) −1.000, (c) −1.020, (d) −1.040 and (e) −1.060 V.

Table 2. Parameters used for current transient fitting according to Equation 12 as shown in Fig. 9 (full traces)

E_f /V	P_1^* /mA cm^{-2} s^{-1}	P_2^* /s^{-2}	P_3 /mA/cm^{-2}	P_4 /s^{-1}	P_5 /s
$E_i = -0.76$ V, $\tau = 3$ s, 1 M NaOH					
−1.06	250.8	44.8	4.32	1.63	0.057
−1.04	216.8	43.8	5.11	2.15	0.052
−1.02	162.7	33.2	4.43	1.78	0.056
−1.00	110.6	25.1	4.67	1.86	0.057
−0.98	82.3	19.3	3.86	1.50	0.051

The preceding analysis indicates that the electroreduction of anodically formed cadmium oxide layers is a complex reaction. In principle, it is expected that the corresponding reaction mechanism is consistent with the complex electro-oxidation pathway earlier advanced [6]. The anodization of cadmium in NaOH solutions involves the formation of a hydrous cadmium oxide layer at low anodic potentials whose water content decreases as the potential is set more positively. Furthermore, the generation of soluble Cd species at potentials more positive than $E_{p,I}$ has been established. Therefore, the initial short-range electroreduction current decay fitting the j–t Equation 3 can be associated with the diffusion controlled reversible electroreduction of Cd(II) soluble species yielding a cadmium overlayer on the substrate. This conclusion is consistent with the value of $D_j \simeq 10^{-6}$ cm^2 s^{-1} derived from P_4. The long-range electroreduction process which can be fitted through Equation 2, also involves the electroreduction of thin cadmium oxide layers formed at E_i through a 2D nucleation and growth mechanism under charge transfer control from the Cd(II) species in the oxide film.

4. Conclusions

The analysis of the potentiostatic electroreduction of anodically formed cadmium oxide films has allowed discrimination between the mechanistic contributions related to the entire phase change process and the correlation of kinetic conclusions from the physical model with those previously obtained through voltammetric and optical measurements. The electroreduction process can be explained through a nucleation and growth mechanism involving soluble Cd(II) and passivating anodic species.

The potentiostatic electroreduction current transients were satisfactorily described by the sum of two contributions, one corresponding to an instantaneous nucleation and 2D growth process under charge transfer control and a second term which represents the initial falling current related to an instantaneous nucleation and 2D growth under diffusion control. Data derived from the parameters of the proposed model given in Equation 12, are in good agreement with those previously obtained through other measuring techniques.

Acknowledgements

This research project was financially supported by the Consejo Nacional de Investigaciones Científicas y Técnicas, the Comisión de Investigaciones Científicas de la Provincia de Buenos Aires, and the Fundación Antorchas.

References

[1] P. C. Milner and V. B. Thomas, *in* 'Advances in Electrochemistry and Electrochemical Engineering' (edited by C. W. Tobias), Vol. 5, Interscience, New York (1967) pp. 1–86.
[2] R. J. Lathan and N. A. Hampson, *in* 'Encyclopedia of the Electrochemistry of the Elements' (edited by A. J. Bard), Vol. I, Marcel Dekker, New York (1973) pp, 155–233.
[3] R. D. Armstrong, K. Edmondson and G. D. West, *in* 'Specialist Periodical Reports on Electrochemistry,' Vol. 4, The Chemical Society, London (1974) pp. 18–32.
[4] S. Gross and R. J. Glockling, 'The Cadmium Electrode. A Review of the Status of Research'. Final Report of Boeing Aerospace Company, Document D180-19046-2 (1976).
[5] R. Barnard, *J. Appl. Electrochem.* **11** (1981) 217.
[6] S. B. Saidman, J. R. Vilche and A. J. Arvia, *Electrochim. Acta* **32** (1987) 395.
[7] Y. Duhirel, B. Beden, J. M. Léger and C. Lamy, *ibid.* **37** (1992) 665.
[8] J. O. Zerbino, S. B. Saidman, J. R. Vilche and A. J. Arvia, *ibid.* **34** (1989) 1167; *idem, ibid.* **35** (1990) 605.
[9] S. B. Saidman, J. R. Vilche and A. J. Arvia, *Thin Solid Films* **182** (1989) 185.

[10] C. A. Gervasi, S. R. Biaggio, J. R. Vilche and A. J. Arvia, *Electrochim. Acta* **36** (1991) 2147.
[11] F. E. Varela, L. M. Gassa and J. R. Vilche, *ibid.* **37** (1992) 1119.
[12] S. B. Saidman, J. R. Vilche and A. J. Arvia, *J. Appl. Electrochem.* **18** (1988) 633.
[13] M. Fleischmann and H. R. Thirsk, *J. Electrochem. Soc.* **110** (1963) 688.
[14] H. R. Thirsk and J. A. Harrison, *in* 'A Guide to the Study of Electrode Kinetics', Academic Press, New York (1972) p. 121.
[15] R. D. Armstrong and J. A. Harrison, *J. Electrochem. Soc.* **116** (1969) 328.
[16] S. B. Hall and G. A. Wright, *Corros. Sci.* **31** (1990) 709.
[17] Y. Okinaka, *J. Electrochem. Soc.* **117** (1979) 289.